DALTON
FULL PAPER

Cu(II) ion coordination to the pentadecapeptide model of the SPARC copper-binding site †

Chiara Conato,[a] Wojciech Kamysz,[b] Henryk Kozłowski,*[c] Marek Łuczkowski,[c] Zbigniew Mackiewicz,[b] Piotr Młynarz,‡[d] Maurizio Remelli,*[a] Daniela Valensin[d] and Gianni Valensin[d]

[a] *Dipartimento di Chimica, Università di Ferrara, Via L. Borsari 46, I-44100 Ferrara, Italia. E-mail: rmm@unife.it*
[b] *Faculty of Chemistry, University of Gdansk, Sobieskiego 18/1, 80-952 Gdańsk, Poland*
[c] *Faculty of Chemistry, University of Wrocław, F. Joliot-Curie 14, 50-383 Wrocław, Poland. E-mail: henrykoz@wchuwr.chem.uni.wroc.pl*
[d] *Dipartimento di Chimica, Università di Siena, Via A. Moro, S. Miniato, Siena, Italia*

Received 17th July 2002, Accepted 9th August 2002
First published as an Advance Article on the web 23rd September 2002

SPARC (Secreted Protein, Acidic and Rich in Cysteine) is a matricellular glycoprotein with many biological functions: it mediates the interactions between cells and the extracellular matrix, playing a role in angiogenesis, tumorigenesis, caractogenesis and wound healing. Proteolysis of SPARC gives rise to a number of oligopeptides which can regulate angiogenesis *in vivo* and the biological activity of which has been related to their association with endogenous or exogenous copper ion. Human SPARC consists of three distinct modules. Module II is follistatin-like and contains two copper binding sites, the strongest of which—the cationic region 2 (amino acids 114–130)—contains the sequence Gly–His–Lys. In order to shed more light on the biological role of metal complexes formed by SPARC and its fragments, more information is needed on their stoichiometry, stability and structure in solution. In the present paper a potentiometric and spectroscopic investigation on Cu(II) complexes with the $SPARC_{114–128}$ fragment, protected at both its amino and carboxylic ends, is reported. This peptide (Ac–TLEGTKKGHKLHLDY–NH_2) constitutes a good model to the strong copper-binding site of the protein. The whole experimental data suggest that complex-formation is started by the two His residues, subsequently involving up to three amido nitrogens, as pH increases. The coordination of the two histydyl imidazoles is able to promote amide ionisation in the physiological pH range and this could be the key to the SPARC affinity for Cu(II) ion.

SPARC (Secreted Protein, Acidic and Rich in Cysteine) is a 32 kD calcium-binding protein of the extracellular matrix (ECM), which is expressed by many cell types and belongs to the class of "matricellular" proteins.[1] It mediates cell–matrix interactions without covering any primarily structural role:[2,3] it is a counter-adhesive protein, it modulates the activity of some growth factors and influences the cell-cycle. SPARC is the product of a single-copy gene and its sequence has been highly conserved during vertebrate evolution and among species, with the mammalian, amphibian and avian proteins showing more than 70% amino acid identity.[4] SPARC is highly expressed during embryonic development while its expression in the adult is generally associated with changes in cell–matrix or cell–cell interactions, as happens during tissue remodelling or renewal and also in response to an injury. It has also been reported that SPARC production is increased in some tumours[5] and SPARC has been proposed as a diagnostic marker of invasive meningiomas.[6] These findings have been associated with the activity of SPARC and of its fragments in angiogenesis,[7] the latter being a fundamental requirement for tumour development. It is worth noting at this point that a high angiogenic activity most often requires high levels of copper, the reduction of which in the body has been recently suggested as a therapeutic tool to control cancer growth.[8] In this context, the interactions between copper ion and SPARC protein (and its fragments) assume particular interest.

The human protein consists of 286 amino acids, which can be divided into three distinct modules; the structure of the last two modules has been recently solved.[9] The N-terminal module (residues 1–52, after a 17 amino acid signal sequence) is an acidic region, which binds 5–8 calcium ions with low affinity. This first module binds to hydroxyapatite, being involved in the mineralization of cartilage and bone. Invertebrate SPARC does not have this ability, developed for a specific function peculiar for vertebrates, *i.e.* bone formation. The second module is a Cys-rich, follistatin-like (FS) domain (residues 53–137), in which all the 10 Cys residues are disulfide-bonded and where a carbohydrate moiety is N-linked at Asn99. This module contains two bioactive peptides (peptide 2.1, residues 55–74; peptide 2.3, residues 114–130), which proved to be responsible for the ability of SPARC to bind copper ion[10] without any competition with the Ca^{2+} binding sites. In particular, the latter fragment, the strongest Cu(II) binding site, contains the sequence Gly–His–Lys (GHK) (residues 121–123). GHK, a well recognised Cu(II) binding peptide, is better known as a liver-cell growth factor; Cu(II)/GHK complexes have been proven to have angiogenic activity and to play an important role in wound healing.[11] Sage and co-workers[10] demonstrated that the residue His_{122} (bearing to the GHK sequence) makes a significant contribution to the SPARC affinity for copper ion; in fact, the Cu(II) binding ability of the $SPARC_{114–130}$ fragment is partially lost on substituting this amino acid with arginine. Peptide 2.3 also contains the sequence KGHK; both KGHK

† Electronic supplementary information (ESI) available: tables of ^{1}H- and ^{13}C-NMR chemical shifts and thermodynamic parameters for Ac–TLEGTKKGHKLHLDY–NH_2; ^{1}H-NMR spectra and a plot of the temperature dependence of R_{1p} for Ac–TLEGTKKGHKLHLDY–NH_2; a proposed structure for Cu(II)/Ac–TLEGTKKGHKLHLDY–NH_2 at pH 10.4. See http://www.rsc.org/suppdata/dt/b2/b207029d/

‡ On leave as a research associate at the Departimento di Chemica, Università di Siena. Funded by the CIRMMP Consortium, CERM, Florence, Italy.

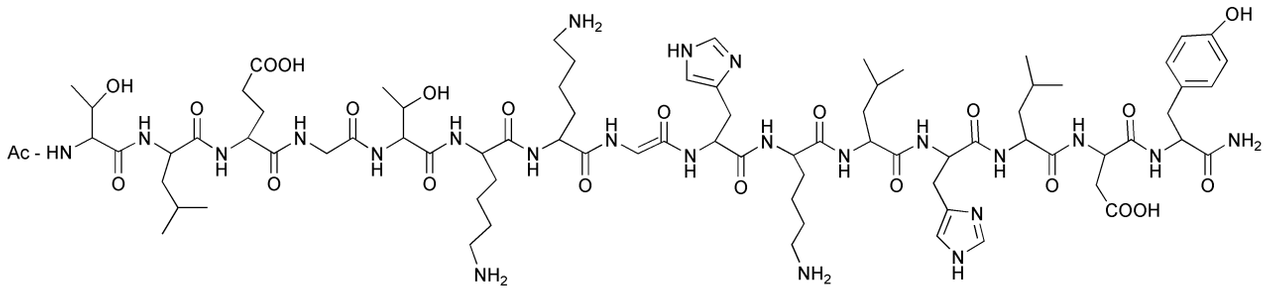

Fig. 1 Structure of the ligand, Ac–TLEGTKKGHKLHLDY–NH_2.

and longer peptides containing this sequence and deriving from the proteolysis of SPARC have been recognised to regulate angiogenesis *in vitro* and *in vivo*.[10] The complex-formation equilibria of GHK and KGHK with Cu(II) have been recently revisited.[12,13] Module III (residues 138–286) is largely α-helical and contains the extracellular high-affinity calcium binding sites. It is globular and contains two EF-hand motifs.

In the present paper, the complex-formation equilibria of the pentadecapeptide Ac–TLEGTKKGHKLHLDY–NH_2 (Fig. 1), corresponding to the $SPARC_{114–128}$ fragment, with the Cu(II) ion have been investigated, at I = 0.1 mol dm^{-3} (KNO_3) and T = 298.2 K. Protonation and complex-formation constants have been potentiometrically determined; formation enthalpies have been measured by direct solution calorimetry; the complex-formation model and species stoichiometry have been carefully checked by means of UV-VIS absorption, CD and EPR spectroscopies. Structure hypotheses for the complex species have been suggested with the aid of a detailed study of the ^{1}H-NMR spectrum of the ligand both in the absence and in the presence of Cu(II).

Experimental

Ac–TLEGTKKGHKLHLDY–NH_2 was manually synthesized on a 0.1 mmol scale by the solid phase method using the Fmoc/Bu^t amino acids,[14,15] according to the following procedure: (i) 5 and 15 min deprotection steps using 20% piperidine in DMF in the presence of 1% Triton; (ii) coupling reactions carried out with the protected amino acid diluted in a mixture of DMF–NMP (*N*-methylpyrrolidone) (1 : 1, v/v) in the presence of 1% Triton, using DIC (1,3-diisopropylcarbodiimide) as the coupling reagent in the presence of HOBt (Fmoc-AA : DIC : HOBt 1 : 1 : 1) for 1.5 h. The completeness of each coupling reaction was monitored by chloranil and ninhydrin tests.[16] The protected peptidyl resin was treated with the mixture: 95% trifluoroacetic acid (TFA), 2.5% water and 2.5% TIS (triisopropylsilane) for 1 h. The cleaved N-Ac-peptide amide was precipitated with diethyl ether and lyophilized. Peptides were purified by solid phase extraction (SPE). The product was homogeneous by TLC and was judged to be more than 98% pure by HPLC. The molecular weight was checked by FAB MS, using an AMD-604 spectrometer. The ion source was equipped with a Cs^+ gun. The energy of the Cs^+ ions was 12 keV.

Aliquots (2.5 cm^3) of sample solution, containing suitable amounts of the metal ion, the ligand, HNO_3 (when the initial pH value needed to be lowered) and KNO_3 (to adjust the ionic strength to 0.1 mol dm^{-3}) were potentiometrically titrated with standard NaOH in a thermostatted potentiometric vessel (pH range = 3.5–11.0; T = 298.2 K). Metal ion concentration was close to 1×10^{-3} mol dm^{-3} and metal to ligand ratio was 1 : 1.2. Two pairs of potentiometric titrations, both for protonation and complex-formation were performed. Further experimental details, equipment and software used are reported elsewhere.[17] Thermodynamic data are given with the estimated accuracy reported as the uncertainty on the last significant figure.

CD, EPR and UV-VIS spectra were recorded on a JASCO J 715, on a Bruker ESP 300E (at 120 K and 9.4 GHz) and on a Beckman DU 650 spectrometer, respectively. Sample solutions had the same composition as above; pH was varied by addition of suitable amounts of standard NaOH or HCl, under potentiometric control. Spectra were recorded every 0.5 pH units.

Calorimetric titrations were performed by means of an Isoperibolic Calorimeter (Tronac) at 298.2 K, by addition of standard HNO_3 to a sample solution (2.5 cm^3) of the same composition as above. For each system two pairs of calorimetric titrations containing not less than 250 experimental points were utilised to calculate the thermodynamic quantities.

NMR spectra were performed at 14.1 T with a Bruker Avance 600 MHz spectrometer at controlled temperatures (±0.1 K). Two different peptide solutions were prepared: the first with deionized water containing 10% D_2O the second with deuterium oxide (99.95% from Merck), and they were carefully deoxygenated through a freeze/pump/seal/thaw procedure. The pH was adjusted to desired values with either DCl or NaOD. The desired concentration of copper ions was achieved by using a stock solution of copper nitrate (Sigma Chemical Co.) in deuterium oxide. TSP-d_4, 3-(trimethylsilyl)-[2,2,3,3-d_4] propanesulfonate, sodium salt, was used as internal reference standard. The assignment was accomplished with TOCSY, COSY, and NOESY 2D experiments. TOCSY spectra were recorded with a total spin-locking time of 75 ms using a MLEV-17 mixing sequence; NOESY spectra were obtained with standard pulse sequences at values of the mixing time ranging between 50 and 400 ms. During all 2D experiments, water suppression was achieved by means of the Watergate method.[18] The spectral width of homonuclear 2D experiments was typically 6000 Hz in both F_1 and F_2 dimensions. Spin–lattice relaxation rates were measured with inversion recovery pulse sequences. The same sequence was also used to measure the single- or double-selective relaxation rates by means of suitably shaped π-pulses instead of the usual non-selective π-pulse. All rates were calculated by regression analysis of the initial recovery curves of longitudinal magnetization components leading to errors not larger than ±3%. 2D ^{1}H–^{13}C shift correlation methods were used to detect and assign ^{13}C-NMR spectra at relatively low concentration. HMBC (multiple-bond heteronuclear multiple-quantum coherence) spectra were obtained with standard pulse sequences, over a spectral width of 6000 Hz in the F_2 dimension and 31700 Hz in the F_1 dimension; a total of 1024 points were used in F_2 and 256 in F_1 which was zero filled once before processing; eight transients were accumulated with a relaxation delay of 2.0 s for each of the 256 increments.

A 5 mm broad band probe was used to perform the ^{13}C-NMR spectra. They were acquired with a FID composed of 32768 data points over a spectral width of 28700 Hz (acquisition time 0.570 s), a 90° pulse of 8.5 μs, relaxation delay of 5.0 s; WALTZ16 broad band decoupling method was used.[19,20]

Molecular structures were generated by the HYPERCHEM software package[21] implemented on a Pentium 120 MHz PC by using the ZINDO-1 semi-empirical method for charge calculations and the MM+ force field for molecular mechanics and dynamics calculations.

Table 1 Protonation constants for Ac–TLEGTKKGHKLHLDY–NH_2, at 298.2 K and $I = 0.1$ mol dm^{-3} (KNO_3)

Species	Residue	log β	log K
HL	Lys	11.19(2)	11.2
H_2L	Lys	21.59(3)	10.4
H_3L	Lys	31.68(3)	10.1
H_4L	Tyr	41.07(4)	9.4
H_5L	His	47.74(4)	6.7
H_6L	His	53.58(4)	5.8
H_7L	Glu	57.77(3)	4.2
H_8L	Asp	61.17(3)	3.4

Table 2 Complex-formation constants in the binary system Cu(II)/Ac–TLEGTKKGHKLHLDY–NH_2, at 298.2 K and $I = 0.1$ mol dm^{-3} (KNO_3)

Species	log β	log K	log K*	Donor set
CuH_5L	52.04(2)		−1.6	1N
CuH_4L	47.14(2)	4.9	−6.5	2N
CuH_3L	40.14(3)	7.0	−13.5	3N
CuH_2L	33.18(2)	7.0	−20.4	4N
CuHL	24.49(2)	8.7	−23.2	4N
CuL	14.77(2)	9.7		4N
$CuH_{-1}L$	4.61(3)	10.2		4N
$CuH_{-2}L$	−6.12(4)	10.7		4N
$CuH_{-3}L$	−17.44(6)	11.3		4N

log K* = log $\beta(CuH_jL)$ − log $\beta(H_nL)$ ($n = 6$ when $j = 2, 3, 4, 5$; $n = 5$ when $j = 1$).

Results

Ligand protonation constants are shown in Table 1 while the complete set of thermodynamic data for ligand protonation is reported in the ESI. It is relatively easy to assign the three first protonation steps to the ε-amino groups of Lys residues, the fourth to the phenolic hydroxyl of Tyr, the fifth and sixth to His imidazoles, and the seventh and eighth to the carboxylic side groups of Glu and Asp, respectively. Within experimental error these results are in good agreement with literature data on analogous ligands.[22]

Table 2 shows the complex-formation constants with the Cu(II) ion while the whole set of thermodynamic parameters is available in the ESI. Nine species have been detected in the explored pH range; all of them are mono-complexes with a different degree of protonation. The distribution diagram reported in Fig. 2 shows that the ligand starts to bind Cu(II) ion

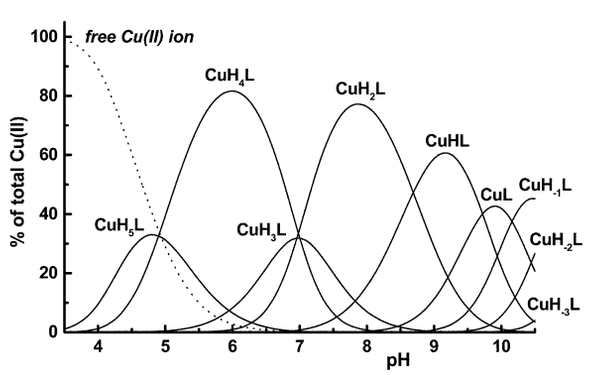

Fig. 2 Distribution diagram of Cu(II)/Ac–TLEGTKKGHKLHLDY–NH_2 complexes. [Cu(II)] = 1.0×10^{-3} mol dm^{-3}, [Ac–TLEGTKKGHKLHLDY–NH_2] = 1.2×10^{-3} mol dm^{-3}, $T = 298.2$ K, $I = 0.1$ mol dm^{-3} (KNO_3).

at a pH value lower than 4, forming first the complex CuH_5L and then the species CuH_4L which dominates the acidic pH range. At physiological pH the three species CuH_4L, CuH_3L and CuH_2L are simultaneously present in comparable amounts.

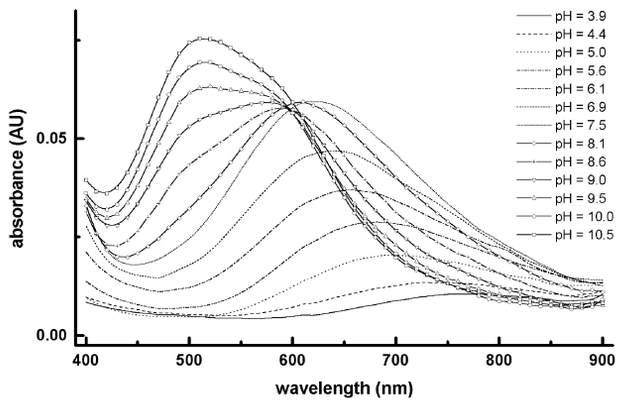

Fig. 3 Absorption spectra of Cu(II)/Ac–TLEGTKKGHKLHLDY–NH_2 solutions. [Cu(II)] = 1.0×10^{-3} mol dm^{-3}, [Ac–TLEGTKKGHKLHLDY–NH_2] = 1.2×10^{-3} mol dm^{-3}, $T = 298.2$ K, $I = 0.1$ mol dm^{-3} (KNO_3).

Electronic spectra (Fig. 3) show that the wavelength of maximum absorption at pH 4 is already lower than that corresponding to the aqueous Cu(II) ion. As pH increases up to pH 8 this band continuously shifts towards lower wavelength values. This behaviour should be due to the coordination of successive nitrogen atoms to the metal ion. Starting from pH 8.5 on a new absorption band appears in the spectrum at 520 nm: it becomes more and more intense as pH increases. The band at 600 nm is still detectable at pH 10.5, as a shoulder, suggesting the presence in solution of at least two complexes with different geometries.

CD spectra show four distinct absorption bands (Fig. 4 and

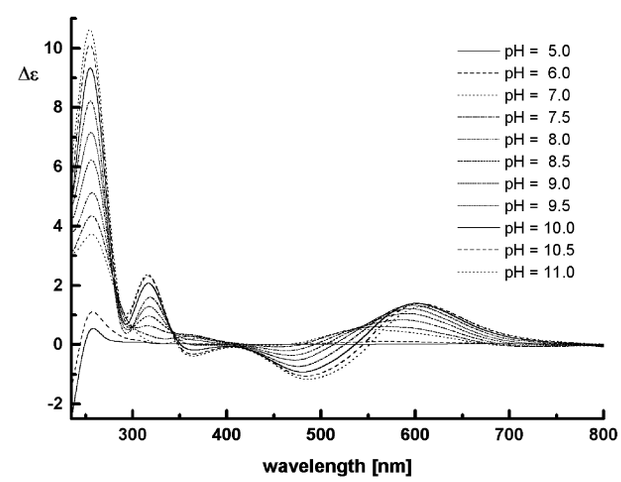

Fig. 4 Circular dichroism spectra of Cu(II)/Ac–TLEGTKKGHKLHLDY–NH_2 solutions. [Cu(II)] = 1.0×10^{-3} mol dm^{-3}, [Ac–TLEGTKKGHKLHLDY–NH_2] = 1.2×10^{-3} mol dm^{-3}, $T = 298.2$ K, $I = 0.1$ mol dm^{-3} (KNO_3).

Table 3). A double band is present in the d–d region, from pH 6 on, which is typical of Cu(II)/His coordination.[23] The two bands at 256 and 364 nm can be ascribed to a CT transition from imidazole π_2 and π_1 to copper, respectively.[24] The positive band at 317 nm is most likely due a CT transition from a deprotonated amidic nitrogen to copper:[24] this band is clearly detected at pH higher than 7.0.

$A_{\parallel}$ and $g_{\parallel}$ parameters are reported in Table 3. At pH = 5 they assume the typical values of a 2N complex; at pH = 7 those of a 3N complex. In the pH range 8.5–9.5, $A_{\parallel}$ increases while $g_{\parallel}$ slightly decreases, suggesting the coordination of a further N atom, possibly in an axial position. From pH 9.5 EPR data become those typical of a 4N complex characterized by a strong ligand field. Such results completely agree with the above electronic spectra in the same pH range.

Table 3 Spectroscopic parameters of Cu(II)/Ac–TLEGTKKGHKLHLDY–NH_2 binary-complex formation, at 298.2 K and I = 0.1 mol dm^{-3} (KNO_3)

pH	UV-VIS λ/nm (ε/M^{-1} cm^{-1})	CD λ/nm ($\Delta\varepsilon$/M^{-1} cm^{-1})	EPR $A_{\parallel}$ ($g_{\parallel}$)
4.0	786 (20)	—	120 (2.33)
5.0	698 (39)	258 (0.55)	120 (2.42); 165 (2.31)
6.0	672 (59)	257 (1.10); 567 (0.11)	162 (2.30)
6.5	651 (75)	256 (2.14); 369 (0.07); 552 (0.25)	165 (2.30)
7.0	626 (100)	256 (3.72); 367 (0.20); 446 (−0.02); 549 (0.51)	162 (2.30); 172 (2.24)
7.5	616 (122)	256 (4.34); 362 (0.16); 454 (−0.07); 565 (0.60)	175 (2.24)
8.0	603 (126)	257 (5.13); 315 (0.15); 358 (0.06); 463 (−0.20); 587 (0.83)	172 (2.23)
8.5	507 (96); 589 (128)	256 (6.22); 317 (0.50); 468 (0.36); 591 (1.05)	186 (2.22)
9.0	507 (117); 577 (133)	256 (7.15); 317 (0.89); 472 (−0.52); 595 (1.21)	186 (2.22)
9.5	518 (135); 562 (138)	255 (8.22); 318 (1.42); 476 (−0.74); 597 (1.33)	207 (2.19)
10.0	521 (145); 566 (141)	255 (9.33); 316 (1.64); 365 (−0.17); 480 (−0.93); 601 (1.39)	210 (2.18)
10.5	519 (157); 566 (147)	254 (10.12); 316 (1.80); 364 (−0.32); 484 (−1.07); 605 (1.38)	210 (2.18)
11.0	519 (163)	254 (10.63); 316 (1.78); 364 (−0.39); 486 (−1.17); 609 (1.28)	210 (2.18)
11.5	520 (168)	255 (10.54); 315 (1.50); 364 (−0.30); 486 (−1.18); 616 (1.01)	210 (2.18)

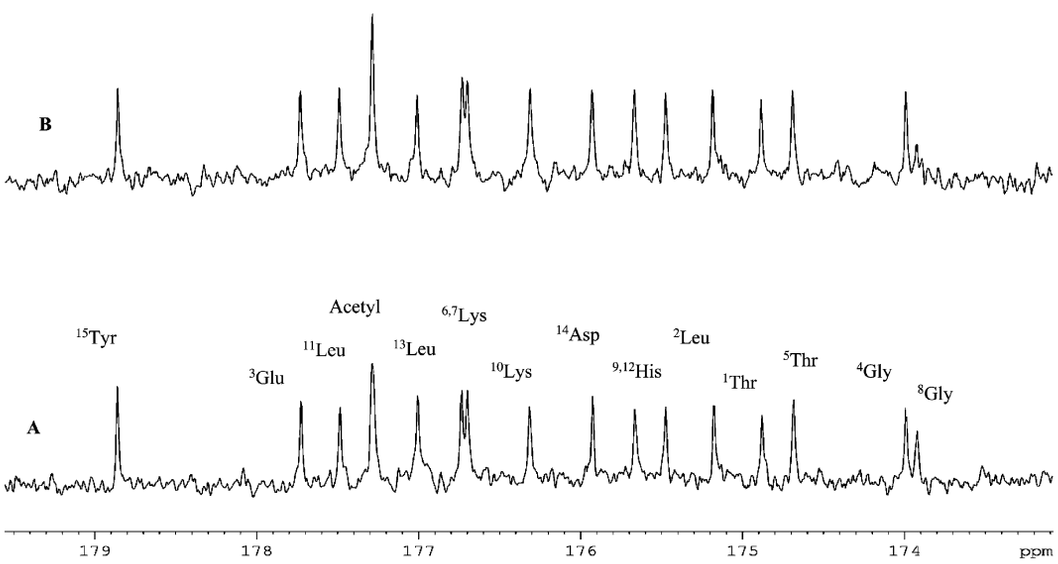

Fig. 5 Low field region of the ^{13}C-NMR spectrum of Ac–TLEGTKKGHKLHLDY–NH_2 (3.8×10^{-3} mol dm^{-3} in D_2O at pH 10.4) before (A) and after (B) the addition of Cu(II) (7.6×10^{-5} mol dm^{-3}).

It is worth noting that above pH 10 four deprotonation steps ($CuHL \longrightarrow CuL + H^+ \longrightarrow CuH_{-1}L + H^+ \longrightarrow CuH_{-2}L + H^+ \longrightarrow CuH_{-3}L + H^+$, see distribution diagram in Fig. 2) can be observed, accompanied by only negligible changes in the spectroscopic parameters. The corresponding thermodynamic parameters (Table 2 and ESI) are close to those measured for the last protonation steps of the free ligand (see Table 1).

The ^{1}H- and ^{13}C-NMR data are reported in the ESI. The low field region of the ^{13}C-NMR spectrum is shown in Fig. 5. When raising the pH from 5.6 to 10.4 most amide protons were washed out from the spectrum by chemical exchange. NMR studies at pH 10.4 were therefore carried out in 99.95% deuterium oxide.

All pertinent NMR data (temperature coefficients of the chemical shifts of amide protons, intramolecular NOEs and HN–Hα coupling constants) were consistent with the absence of secondary structure elements. Moreover, the concentration dependence of chemical shifts indicates a negligible self-aggregation in the studied range.

Addition of copper to the investigated system selectively determines shift, line broadening and enhancement of spin–lattice relaxation rates.

With respect to what is usually encountered with Cu(II), relatively large metal : ligand ratios could be achieved before measuring sizeable relaxation effects, especially at the higher pH. The comparison of the proton NMR spectra of the metal-free peptide with that in the presence of Cu(II) at pH 5.6 indicates that only imidazole protons of ^{9}His and ^{12}His are selectively broadened. The presence of Cu(II) ions also distinctly affects the relaxation rates of imidazole and β protons of both His residues and the amide proton of ^{11}Leu. Some small although clear changes are seen on the relaxation rates of the protons of ^{14}Asp and ^{13}Leu (Fig. 6).

The exchange regime occurring at pH 10.4 does not allow us to follow the signal broadening. The relaxation rates, however, indicate the most distinct changes on the ^{9}His protons and a slight variation for the protons of ^{3}Glu, ^{7}Lys, ^{14}Asp and ^{15}Tyr (Fig. 7).

Selective broadening detected in several regions of the ^{13}C-NMR spectrum (Figs. 5 and 8) indicates that copper perturbs other molecular regions beyond His, namely the ^{8}Gly carbonyl and Cε and Cδ of ^{7}Lys residues. Overlapped ^{13}C-NMR spectra do not allow, however, distinction between the ^{9}His and ^{12}His residues.

Discussion

On the basis of the experimental results reported above, the following hypotheses on the structure of the species formed in the Cu(II)/Ac–TLEGTKKGHKLHLDY–NH_2 system can be proposed.

The species detected at the most acidic pH value—the complex CuH_5L—most likely is a 1N species, where the Cu(II) ion is bound to an imidazole nitrogen; no data are available regarding

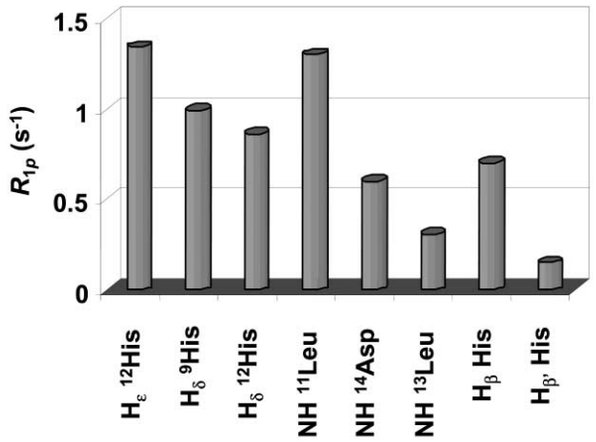

Fig. 6 R_{1p} values measured for selected protons of Ac–TLEGTKKGHKLHLDY–NH_2 (2.2×10^{-3} mol dm^{-3} in D_2O–H_2O at pH 5.6) after the addition of Cu(II) (8.8×10^{-6} mol dm^{-3}). Concerning the β and β′ protons the two His residues are indistinguishable.

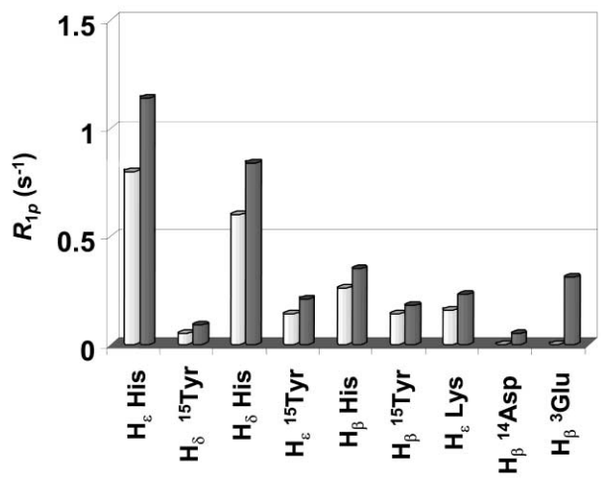

Fig. 7 R_{1p} values measured for selected protons of Ac–TLEGTKKGHKLHLDY–NH_2 (3.8×10^{-3} mol dm^{-3} in D_2O at pH 10.4) after the addition of copper. Dark bar: [Cu(II)] = 1.9×10^{-4} mol dm^{-3}; light bar: [Cu(II)] = 7.6×10^{-5} mol dm^{-3}. The two His and the three Lys residues are indistinguishable; β and β′ protons have the same R_{1p}.

which of the two His residues is favoured for the coordination. A mixture of the two structures, which should have similar thermodynamic and spectroscopic characteristics, can be suggested. The complex stoichiometry requires that both the Asp and Glu residues are not protonated. The computed step constant log β_{CuH_3L} − log K_{H_3L} = 4.3 (see Table 2), corresponding to the coordination of a protonated ligand to the Cu(II) ion, is very close to that reported for the Cu(II)/imidazole system (4.2), under the same experimental conditions.[22] Electronic and EPR spectra in the pH range 4.0–5.0 agree with this hypothesis, taking into account the fact that a high percentage of free copper ion is also present. CD spectra are not very intense, but the band at 258 nm is clearly visible, in agreement with the above structural hypothesis.

EPR an UV-VIS data at pH 6 (where the CuH_4L species reaches its highest concentration) clearly denote a 2N complex. There are two main possibilities: (1) the Cu(II) ion promotes the deprotonation of one amido nitrogen; (2) the second imidazole binds the Cu(II) ion, thus forming a macrochelate ring of 17–19 atoms (depending on which N atoms of the imidazole groups are used). The $\log K_{CuH_4L}^{CuH_3L}$ value (= 4.9, see Table 2) rules out the coordination of a Lys residue. That value instead agrees with both the above hypotheses, being slightly lower than the value log *K* corresponding to the protonation of the second His

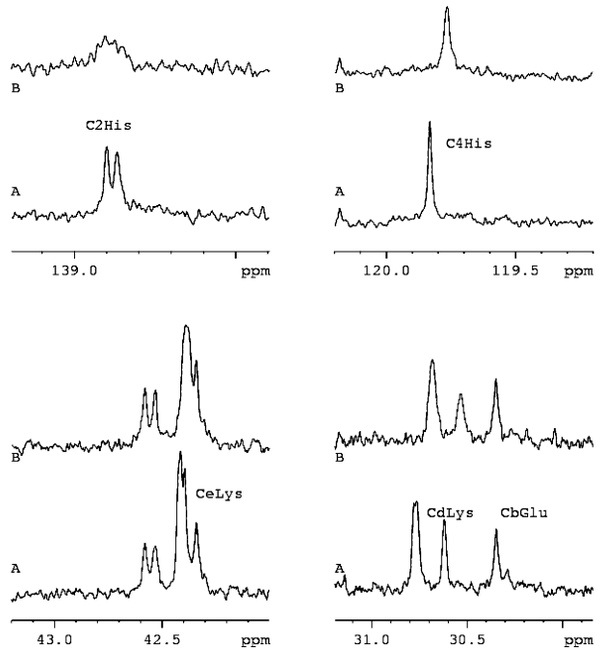

Fig. 8 Selected regions of the ^{13}C-NMR spectrum of Ac–TLEGTKKGHKLHLDY–NH_2 (3.8×10^{-3} mol dm^{-3} in D_2O at pH 10.4) before (lower traces) and after (upper traces) the addition of Cu(II) (7.5×10^{-5} mol dm^{-3}).

residue, but also close to the literature values regarding the first amide deprotonation/coordination of simple oligopeptides.[22] However, in the latter cases, the transition from the 1N to the 2N species corresponds to the substitution of the carbonyl oxygen with the amido nitrogen of the first peptide bond. On the contrary, with the protected tetrapeptide Boc–Ala–Gly–Gly–His[25] the corresponding log *K* value is 6.8, *i.e.* notably higher than here; in that case only His can initiate the coordination and only the amido nitrogen can bind copper to form the 2N species. Moreover, CD spectra do not show the characteristic N_{amido}–Cu(II) CT band below pH 7.5, although it is worth underlying that this absence is only a clue, not proof, of the absence of a N_{amido}–Cu(II) bond. The whole of these observations leads to the hypothesis that in this 2N complex the two imidazole nitrogens simultaneously bind the copper ion.

As pH increases from 6.0 to 8.0 the complex loses two protons and the most abundant species at pH 8, *i.e.* the CuH_2L complex, is formed. Such deprotonation steps are characterized by identical log*K* values (7.0, see Table 2), which are compatible with the deprotonation of two amido nitrogens, promoted by copper (see above). The same was already suggested for other protected peptides containing one or more His residues.[25–28] The high similarity of these two p*K* values suggests that the two deprotonation/complexation steps involve two nearly equivalent donor atoms. The above observations lead to the following structure hypothesis for the CuH_2L complex: the ligand behaves in a tetradentate fashion, with two $N_{imidazole}$ and two amido nitrogens bound to Cu(II). The spectroscopic data, closer to those characteristic of a 3N than of a 4N species, suggest that one of the $N_{imidazole}$ atoms is axially coordinated.

Starting from pH 8.5 on, in the pH range where the CuHL complex becomes the main species in solution, the UV-VIS spectra show a well defined new shoulder located around 515 nm, evolving to an intense absorption band at higher pH. EPR spectra, from pH 9.0–9.5 on, are typical for a Cu(II) complex bearing four nitrogens as donor atoms in the main equatorial plane. The corresponding p*K* value (log β_{CuH_2L} − log β_{CuHL} = 8.7) is compatible with the coordination of a further amido nitrogen to the copper ion. The big changes in the spectroscopic properties suggest a rearrangement in the complex structure: one imidazole and three adjacent amido

nitrogens being bound in the equatorial plane, with a possible axial interaction by the second imidazole ring.

Finally, the further complexes found at higher pH values (the CuL, $CuH_{-1}L$, $CuH_{-2}L$ and $CuH_{-3}L$ species, see Fig. 2) most likely simply derive from the CuHL complex through subsequent deprotonations of the basic side group of Tyr and Lys residues, which do not seem to participate in Cu(II) coordination.

The effect of paramagnetic copper(II) on spin–lattice relaxation rates is measured by the R_{1p} value defined as:

$$R_{1p} = R_{1m} - R_{1f}$$

where R_{1f} and R_{1m} are the rates calculated in the absence and in the presence of the metal, respectively. Since the ligand occurs in the bulk and in the metal coordination sphere, consideration of exchange yields:[29]

$$R_{1p} = \frac{p_b}{R_{1M}^{-1} + k_{off}^{-1}}$$

where k_{off} is the kinetic constant for dissociation from the bound state and p_b is the fraction of bound ligand, the relaxation of which being described by R_{1M}. R_{1M} is usually accounted for by the Solomon equation[30] and it is proportional to the inverse sixth power of the metal–nucleus distance. Raising the temperature obviously increases k_{off}. Thus, only when R_{1p} decreases with raising the temperature, can the contribution of exchange be excluded. The temperature dependence measured for His protons at pH 5.6 (see ESI) shows the occurrence of an intermediate exchange region where $k_{off} \cong R_{1M}$. This is likely to be the reason why high metal : ligand ratios can be reached without severe alteration of the NMR spectra.

Although the NMR data are obtained for high excess of ligand and they cannot be directly transferred to the equimolar solutions discussed above the distinct effect of Cu(II) ions on the protons of both His residues (see Fig. 6 and ESI) strongly support the involvement of two imidazoles in metal coordination at physiological pH. The macrochelate formed with two imidazole nitrogens bound to Cu(II) may interact with the negatively charged carboxylate of the adjacent ^{14}Asp residue.

At pH 10.4 ratios as high as 1 : 50 or 1 : 20 can be reached: this result is consistent with slower off-rates arising from a more complicated exchange process. The observed spin–lattice relaxation rate enhancements (Fig. 7) and line broadenings observed on the ^{13}C-NMR spectra (Fig. 8) suggest that copper is bound to ^{9}His and the coordination takes place in the N-terminal direction, thus involving the ^{8}Gly and ^{7}Lys residues. These conclusions agree very well with the structural hypotheses discussed above.

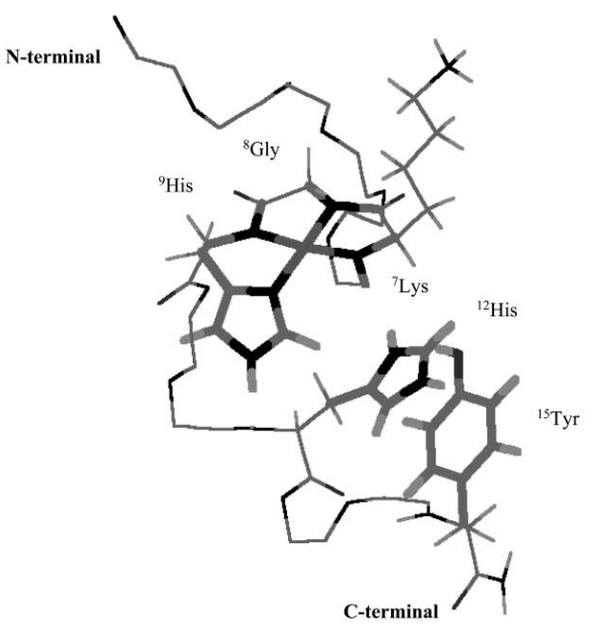

Fig. 9 Structure hypothesis for the Cu(II)/Ac–TLEGTKKGHKLHLDY–NH_2 complex at pH 10.4.

Moreover the effects measured on R_{1p} of ^{12}His, ^{14}Asp and ^{15}Tyr may result from the accumulation of the negative charges on the C-terminal side of the peptide (Tyr–O^-, Asp–CO_2^-) and their proximity to a paramagnetic centre. In addition, molecular mechanics calculations[21] performed on the Cu(II)/Ac–TLEGTKKGHKLHLDY–NH_2 complex with the suggested $\{3N^-, N_{imid}\}$ donor set (alkaline pH range) gave low energy structures (see Fig. 9) where ^{12}His is very close to the metal centre. The obtained data also suggest a stacking interaction between the imidazole of ^{12}His and the phenolate of ^{15}Tyr.

Acknowledgements

Financial support from the Italian MURST (COFIN '98), Polish State Committee for Scientific Research (KBN 4 TO9A 054 23) and the University of Gdansk (BW-8000-5-0319-1) is gratefully acknowledged.

References

1 P. Bornstein, *Matrix Biol.*, 2000, **19**, 555.
2 R. A. Brekken and E. H. Sage, *Matrix Biol.*, 2000, **19**, 569.
3 A. D. Bradshaw and E. H. Sage, *J. Clin. Invest.*, 2001, **107**, 1049.
4 Q. Yan and E. H. Sage, *J. Histochem. Cytochem.*, 1999, **47**, 495.
5 T. F. Lane and E. H. Sage, *FASEB J.*, 1994, **8**, 163.
6 S. A. Rempel, S. Ge and J. A. Gutierrez, *Clin. Cancer Res.*, 1999, **5**, 237.
7 E. H. Sage, *Nature Med.*, 1997, **3**, 144.
8 G. J. Brewer, *Exp. Biol. Med.*, 2001, **226**, 665.
9 E. Hohenester, P. Maurer and R. Timpl, *EMBO J.*, 1997, **16**, 3778.
10 T. F. Lane, M. L. Iruela-Arispe, R. S. Johnson and E. H. Sage, *J. Cell Biol.*, 1994, **125**, 929.
11 L. Pickart, J. Freedman, W. J. Loker, J. Peisach, C. M. Perkins, R. E. Stenkamp and B. Weinstein, *Nature*, 1980, **288**, 715.
12 C. Conato, R. Gavioli, R. Guerrini, H. Kozłowski, P. Młynarz, C. Pasti, F. Pulidori and M. Remelli, *Biochim. Biophys. Acta*, 2001, **1526**, 199 and references therein.
13 C. Conato, H. Kozłowski, P. Młynarz, F. Pulidori and M. Remelli, *Polyhedron*, 2002, **21**, 1469.
14 R. B. Merrifield, *J. Am. Chem. Soc.*, 1963, **85**, 2149.
15 G. Barany and R. B. Merrifield, in *The peptides: Analysis, Synthesis, Biology*, eds. E. Gross and J. Meienhofer, Academic Press, New York, 1980, p. 1.
16 J. E. Kaiser, R. C. Colescott, C. A. Bossinger and D. J. Cook, *Anal. Biochem.*, 1970, **34**, 595.
17 M. Remelli, C. Conato, A. Agarossi, F. Pulidori, P. Młynarz and H. Kozłowski, *Polyhedron*, 2000, **19**, 2409.
18 M. Piotto, V. Saudek and J. Sklenàr, *J. Biomol. NMR*, 1992, **2**, 661.
19 A. J. Shaka, J. Keeler and R. Freeman, *J. Magn. Reson.*, 1983, **53**, 274.
20 G. A. Morris and R. Freeman, *J. Magn. Reson.*, 1978, **29**, 433.
21 HYPERCHEM, Hypercube release 5.1 Pro for Windows, 1997, Hypercube Inc., Waterloo, Canada.
22 L. D. Pettit and H. K. J. Powell, *The IUPAC Stability Constants Database*, Academic Software and IUPAC, Royal Society of Chemistry, London, 1992–1997.
23 P. Młynarz, W. Bal, T. Kowalik-Jankowska, M. Stasiak, M. T. Leplawy and H. Kozłowski, *J. Chem. Soc., Dalton Trans.*, 1999, 109.
24 P. G. Daniele, E. Prenesti and G. Ostacoli, *J. Chem. Soc., Dalton Trans.*, 1996, 3269.
25 L. D. Pettit, S. Pyburn, W. Bal, H. Kozłowski and M. Bataille, *J. Chem. Soc., Dalton. Trans.*, 1990, 3565.
26 M. A. Zoroddu, M. Peana, T. Kowalik-Jankowska, H. Kozłowski and M. Costa, *J. Chem. Soc., Dalton. Trans.*, 2002, 458.
27 M. Casolaro, M. Chelli, M. Ginanneschi, F. Laschi, L. Messori, M. Muniz-Miranda, A. M. Papini, T. Kowalik-Jankowska and H. Kozłowski, *J. Inorg. Biochem.*, 2002, **89**, 181.
28 M. Remelli, M. Luczkowski, A. M. Bonna, Z. Mackiewicz, C. Conato and H. Kozłowski, *New J. Chem.*, submitted.
29 T. J. Swift and R. E. Connick, *J. Chem. Phys.*, 1962, **37**, 307.
30 I. Solomon, *Phys. Rev.*, 1955, **99**, 559.